pISSN 1226-9751 / eISSN 2288-3800 http://dx.doi.org/10.13104/jksmrm.2013.17.3.192

Original Article

Dynamic Contrast-Enhanced MR Imaging in Detecting Local Tumor Progression after HIFU Ablation of Localized Prostate Cancer

Jung Jae Park[1], Chan Kyo Kim[1], Hyun Moo Lee[2], Byung Kwan Park[1], Sung Yoon Park[1]

[1]Departments of Radiology and Center for Imaging Science and [2]Urology, Samsung Medical Center, Sungkyunkwan University School of Medicine, Korea

Purpose : To retrospectively evaluate the diagnostic performance of dynamic contrast-enhanced MR imaging (DCE-MRI) in detecting recurrent prostate cancer after HIFU of clinically localized cancer, as compared with T2-weighted imaging (T2WI).

Materials and Methods: Twenty-six patients with increased prostate-specific antigen levels after HIFU were included in this study. All MR examinations were performed using T2WI and DCE-MRI, followed by transrectal ultrasound-guided biopsy. MRI and biopsy results were correlated in six prostate sectors. Residual or recurrent cancer after HIFU was defined as local tumor progression if biopsy results showed any cancer foci. Two independent readers interpreted the MR images.

Results: Of 156 prostate sectors, 51 (33%) were positive for cancer in 17 patients. For detecting local tumor progression, the sensitivity of DCE-MRI and T2WI was 80% and 57% for reader 1 ($P < 0.001$) versus 84% and 61% for reader 2 ($P < 0.001$), respectively. The specificity and overall accuracy between DCE-MRI and T2WI showed no statistical difference in both readers ($P > 0.05$). Interobserver agreement of DCE-MRI and T2WI was moderate and fair, respectively.

Conclusion: For detecting local tumor progression of prostate cancer after HIFU, DCE-MRI was more sensitive than T2WI, with less interobserver variability.

Index words : High intensity focused ultrasound · Localized prostate cancer · Magnetic resonance imaging (MRI) Dynamic contrast-enhanced MRI

INTRODUCTION

Radical prostatectomy remains the standard treatment for patients with localized prostate cancer and a life expectancy exceeding 10 years (1). For patients with a life expectancy of less than 10 years who are not fit for surgery or do not want to experience the potential side effects of surgery, several alternative treatments have been introduced, such as, three-dimensional radiotherapy, brachytherapy, cryotherapy, and high intensity focused ultrasound (HIFU) (2–4).

HIFU can result in coagulation necrosis in targeted tissue by the conversion of mechanical energy into heat and a cavitation effect (5). Currently, HIFU is a valuable alternative for well- and moderately differentiated localized prostate cancer as well as for local recurrence after external beam radiation therapy (6–8). After HIFU for clinically localized prostate cancer, the accurate assessment of residual or recurrent cancer is much important to determine the planning of treatment strategies as second-line treatment.

• Received; March 31, 2013 • Revised; August 14, 2013
• Accepted; August 28, 2013
Corresponding author : Chan Kyo Kim, M.D.
Department of Radiology and Center for Imaging Science, Samsung Medical Center, 50 Ilwon-dong, Gangnam-gu, Seoul 135-710, Korea.
Tel. 82-2-3410-0516, Fax. 82-2-3410-2559
E-mail : chankyokim@skku.edu

After HIFU, prostate tissue is replaced by coagulation necrosis and fibrosis that are less vascular than normal prostate (9, 10). This can offer more favorable conditions for differentiating, using dynamic contrast-enhanced MR imaging (DCE-MRI), residual or recurrent cancers (which is usually hypervascular) from post-HIFU fibrosis (which is rather homogeneous and hypovascular). To date, to our knowledge, only a few investigations for DCE-MRI following HIFU of localized prostate cancer has been published in terms of the early detection of residual or recurrent prostate cancer after HIFU (11–13). Therefore, the purpose of this study was to retrospectively evaluate the diagnostic performance of DCE-MRI in detecting recurrent prostate cancer after HIFU of clinically localized cancer, as compared with T2-weighted imaging (T2WI).

MATERIALS AND METHODS

HIFU Procedure

Transrectal HIFU using an Ablatherm HIFU device (EDAP SA, Lyon, France) with an endorectal firing head that incorporated both a 7.5 MHz ultrasound-imaging probe and a 3 MHz piezoelectric treatment transducer was performed in our institution. Contiguous shots (5 sec on, 5 sec off) were delivered repeatedly to obtain complete treatment of the whole gland, while preserving the rectal wall and the surrounding structures. To protect the external sphincter and neurovascular bundles, a safety margin of about 6 mm was defined for treating both the apex and posterior lobes.

HIFU was performed under spinal anesthesia. A suprapubic catheter was placed preoperatively to sustain adequate urinary drainage. Combined transurethral resection of the prostate (TURP) was undertaken to reduce prolonged urinary retention before HIFU. Immediately after TURP, localization of the targeted volume boundaries was followed and contiguous HIFU shots were delivered slice-by-slice from the apex to the bladder neck to treat the entire prostate. The suprapubic catheter was removed after the test if the postvoid residual urine was less than 50 ml.

Patients

Between March 2004 and July 2006, 74 patients who were diagnosed with clinically localized prostate cancer were treated by transrectal HIFU using the Ablatherm TM device (EDAP SA, Lyon, France) and combined transurethral resection of the prostate was performed. The selected population included patients with clinical stage T1-2, prostate-specific antigen (PSA) level < 30 ng/ml and no evidence of metastasis on preoperative prostate MR imaging and bone scan. All patients were unsuitable for radical prostatectomy because of their age or comorbidities, or were not willing to undergo surgery. The PSA level was assessed 1 month postoperatively, then every 3 months in the first year and every 6 months thereafter. In the case with a rising PSA equal to or exceeding 1.0 ng/ml, PSA was more frequently monitored than the scheduled interval.

Of the 74 patients, 26 (range, 60–82 years; mean age, 67.8 years) who had consecutive or significant increase of the PSA level underwent a follow-up MR imaging to detect recurrent prostate cancer and formed this study group. After MR examinations, all 26 patients performed subsequently transrectal ultrasound (TRUS)-guided prostate biopsy. Before MR examinations, the last mean level of PSA in all patients was 2.97 $\pm$ 2.5 ng/ml (range, 0.42–10.8 ng/ml). The mean interval between HIFU and MR examination was 9.7 $\pm$ 6.9 months (range, 3–26 months). The mean PSA level before HIFU was 7.25 $\pm$ 6.3 ng/ml (range, 0.12–23.5 ng/ml). Of 26 patients, 10 received neoadjuvant hormonal therapy before the visit to our hospital. All hormonal therapy was discontinued at the time of the HIFU.

This study obtained the approval of the institutional review board and informed consent was waived due to retrospective analysis.

MR Imaging

The prostate MR imaging was performed at 3.0 T (Intera Achieva 3T, Philips Medical System, Best, The Netherlands) by using a phased-array (cardiac SENSE, 6 channel) coil. Before scanning, 20 mg of butyl scopolamine (Buscopan, Boehringer, Ingelheim, Germany) was injected intramuscularly to suppress the peristalsis of bowel. No additional bowel preparation was performed. After obtaining three plain localizer

images, T2-weighted turbo spin-echo imaging (T2WI) was acquired in the three orthogonal planes (axial, sagittal, and coronal). Scan parameters of T2WI were as follows: repetition time msec/ echo time msec, 3364–3370/80; slice thickness, 3 mm; interslice gap, 0.3 mm; matrix, 512 × 304; field of view, 18 cm; number of signal acquired, 3; sensitivity encoding factor, 2. Axial T1-weighted turbo spin-echo sequence (4 mm slice thickness) was acquired to assess lymph nodes and pelvic bone.

DCE-MRI was obtained using a 3D-fast field echo sequence in the axial plane (repetition time msec/echo msec, 7.4/3.9; flip angle, 25°; matrix, 224 × 179; slice thickness, 5 mm; interslice gap, no; field of view, 20 cm; 11 partitions on a 3D slab). DCE-MRI was scanned from the apex to base of the prostate. 3D volume with 11 partitions was acquired every 5 sec and a total of 58 were repeated. Dynamic series consisted of one precontrast series and subsequent 57 postcontrast series. Postcontrast series was performed immediately after a bolus injection of gadopentetate dimeglumine (Magnevist, Schering, Germany) at a rate of 2 ml/sec with a dose of 0.1 mmol/kg body weight by using a power injector. A total of acquisition times for DCE-MRI were approximately 5 min 22 sec.

All dynamic data sets were transferred to an independent workstation (ViewForum, Philips Medical System, Best, The Netherlands) to measure the wash-in rate, wash-out rate, maximal enhancement and time to peak and generate parametric imaging of them. Time-signal intensity curves were first fitted to a general exponential signal enhancement model. Dynamic images were converted to a four-parameter model: wash-in rate, wash-out rate, maximal enhancement and time to peak. Wash-in rate is defined as the maximum slope between the time of onset of contrast inflow and the time of peak enhancement on the time-signal intensity curve. Wash-out rate is defined as the negative slope of the late part of the exponential curve. Maximal enhancement is the concentration at which the exponential curve becomes level and the exponential constant defines the time to peak. Postprocessing procedure (about 6 minutes per patient) was performed by a radiologist and the radiologist extracted a threshold value of four parameters that were optimal for differentiating cancer from normal tissue. Then, the radiologist generated parametric imaging using the same threshold for all patients. In parametric imaging, pixels with a wash-in rate, wash-out rate, maximal enhancement and time to peak value greater than the threshold value were color-coded over the enhanced fast-field echo images.

Image Analysis and Transrectal Biopsy

In the follow-up period after HIFU, positive results of prostate biopsy have two meanings (i.e., residual or new-developed recurrent cancer in the remnant prostatic tissues). However, it is virtually impossible to determine whether there was incompletely treated viable tumor that continued to grow or if a new tumor. Hence, in this study, residual or new-developed recurrent prostate cancer was considered as local tumor progression if prostate biopsy results showed any cancer foci (14).

Two readers were asked to identify the presence of cancer in 6 prostate sectors (upper, mid and lower on each lobe). Since HIFU results in morphologic deformities of the prostate with indistinct zonal anatomy, we could not subdivide the prostate into the peripheral zone and central gland.

Two readers reviewed the MR images on a picture archiving and communication system (PathSpeed workstation; GE Medical Systems, Milwaukee, Wis). Two readers (C.K.K., B.K.P.) had more than 5 years of experience in reading prostate MR images. They only knew that the PSA level was rising and were unaware of each other's findings and of the patient data. First, T2WI was independently assessed by two readers without knowledge of the results of DCE-MRI. More than three weeks after the first assessment, two readers evaluated DCE-MRI independently.

The diagnostic criteria of prostate cancer at T2WI and DCE-MRI were as follows: at T2WI, focal or mass-like hypointense area in the remnant prostate tissue was considered as prostate cancer. However, an area of diffusely low-signal intensity relative to the adjacent muscle at T2WI was considered as a fibrotic change due to HIFU. In addition, T2 signal intensity similar to the normal peripheral zone of gland before HIFU was considered as noncancerous tissue. At parametric imaging of DCE-MRI, the presence of asymmetric wash-in rate, wash-out rate, maximal enhancement, and/ or decreased time to peak was highly indicative of prostate cancer (15–17). Quantitative analysis for DCE-

 http://dx.doi.org/10.13104/jksmrm.2013.17.3.192

MRI was not performed.

TRUS-guided biopsy was performed in all 26 patients with an 18-gauge needle mounted on a spring-loaded commercial biopsy device (Biopty Gun; Bard, Covington, Ga., U.S.A.). After a local periprostatic anesthesia, all patients obtained each sextant biopsy cores (upper, mid and lower on each lobe) by two genitourinary radiologists (C.K.K., B.K.P.). At the time of transrectal prostate biopsy, these two radiologists were aware of the MR imaging results and were asked to direct the biopsy carefully toward that part of the sextant whenever he thought a sextant contained a suspicious lesion on MR imaging. All biopsy cores were labeled to identify the biopsy location and all specimens were evaluated by one experienced uropathologist. The mean time interval between MR imaging and biopsy was 22.6 ± 17.9 days (range, 1–75 days). The mean volume of residual prostate tissue was 12 ± 4.3 ml (range, 6–22 ml).

Statistical Analysis

Statistical analysis was performed with a statistical software package (SPSS for Windows, version 18.0; SPSS, Chicago III). The sensitivity, specificity, positive predictive value (PPV), negative predictive value (NPV), and overall accuracy for the detection of recurrent prostate cancer after HIFU were calculated using histopathologic results as a standard of reference. The comparison in the detection of local tumor progression of prostate cancer between T2WI and DCE-MRI was made using McNemar test. The bonferroni correction was used to adjust for multiple comparisons. For the overall accuracy at DCE-MRI and T2WI, generalized estimation equation to account for clustering effects from multiple measurements in the same patient was used.

The interobserver agreement between two readers for the detection of local tumor progression of prostate cancer after HIFU was calculated with nonweighted κ statistics. The following qualitative terms were used to describe the strength of various of κ: 0–0.20, poor agreement; 0.21–0.40, fair agreement; 0.41–0.60, moderate agreement; 0.61–0.80, substantial agreement; and 0.81–1.00, almost perfect agreement (18). Two-tailed tests were used to calculate all P values; a P value of 0.05 or less than was considered to indicate a statistically significant difference.

RESULTS

Biopsies were obtained from 156 sites in 26 patients. At histopathologic findings, local tumor progression was found at 33% (51/156 sectors) of 17 patients. The mean Gleason sum score was 7.0 ± 1.1 (median, 7; range, 6–10).

Table 1 presents the results of DCE-MRI and T2WI for the detection of local tumor progression of prostate cancer in 26 patients after HIFU (Figs. 1, 2). For the detection of local tumor progression of prostate cancer, the sensitivity of DCE-MRI and T2WI were 80% and 57% for reader 1 ($P < 0.001$) versus 84% and 61% for reader 2 ($P < 0.001$), respectively. The specificity of DCE-MRI showed similar results with T2WI ($P = 0.75$). The overall accuracy of DCE-MRI was higher than that of T2WI in both readers, but

Table 1. Diagnostic Performance of Dynamic Contrast-Enhanced Imaging (DCE-MRI) and T2-Weighted Imaging (T2WI) for the Detection of Local Tumor Progression after HIFU Ablation of Localized Prostate Cancer in 26 Patients

	Reader 1		Reader 2	
	DCE-MRI	T2WI	DCE-MRI	T2WI
Sensitivity (%)	80 (41/51)*	57 (29/51)	84 (43/51)*	61 (31/51)
Specificity (%)	63 (66/105)	66 (70/105)	64 (67/105)	68 (71/105)
PPV (%)	51 (41/80)	45 (29/64)	54 (43/80)	48 (31/65)
NPV (%)	87 (66/76)	76 (70/92)	88 (67/76)	78 (71/91)
Accuracy (%)	69 (107/156)	63 (99/156)	71 (110/156)	65 (102/156)

Note.— The parentheses are raw data. PPV = positive predictive value, NPV = negative predictive value.
* Comparison between DCE-MRI and T2WI: P< 0.001

no statistical difference between them was shown (P = 0.142 for reader 1 and P = 0.152 for reader 2).

For the detection of local tumor progression of prostate cancer, the interobserver agreement of DCE-MRI and T2WI was moderate (k = 0.52) and fair (k = 0.21), respectively.

False-positive findings of DCE-MRI on reader 1 and 2 were 10 (20%) and 8 (16%) prostate sectors, respectively, while those of T2WI on reader 1 and 2 were 22 (43%) and 20 (39%) prostate sectors, respectively.

DISCUSSION

Until now, only a few reports on the use of MR imaging for prostate evaluations after HIFU are available (9–13). MRI appearance of prostate following transrectal HIFU of localized cancer and HIFU-induced abnormalities (i.e., on fat-saturated contrast-enhanced T1-weighted images, the HIFU-induced lesion appeared as a nonenhancing hypointense zone surrounded by a 3- to 8-mm thick peripheral rim of enhancement) seem to disappear within 3–5 months (9). Thus, after that period, early enhancing lesion in residual prostate tissue might raise a possibility of residual or recurrent (i.e., local tumor progression) of prostate cancer at DCE-MRI. Thus, in our study, DCE-MRI was assessed for enhancement in the posttreatment field on the basis of the fact that nonenhancement indicated avascularity and therefore cell death, while enhancement indicated residual or recurrent viable prostatic tissue (both normal gland and/or

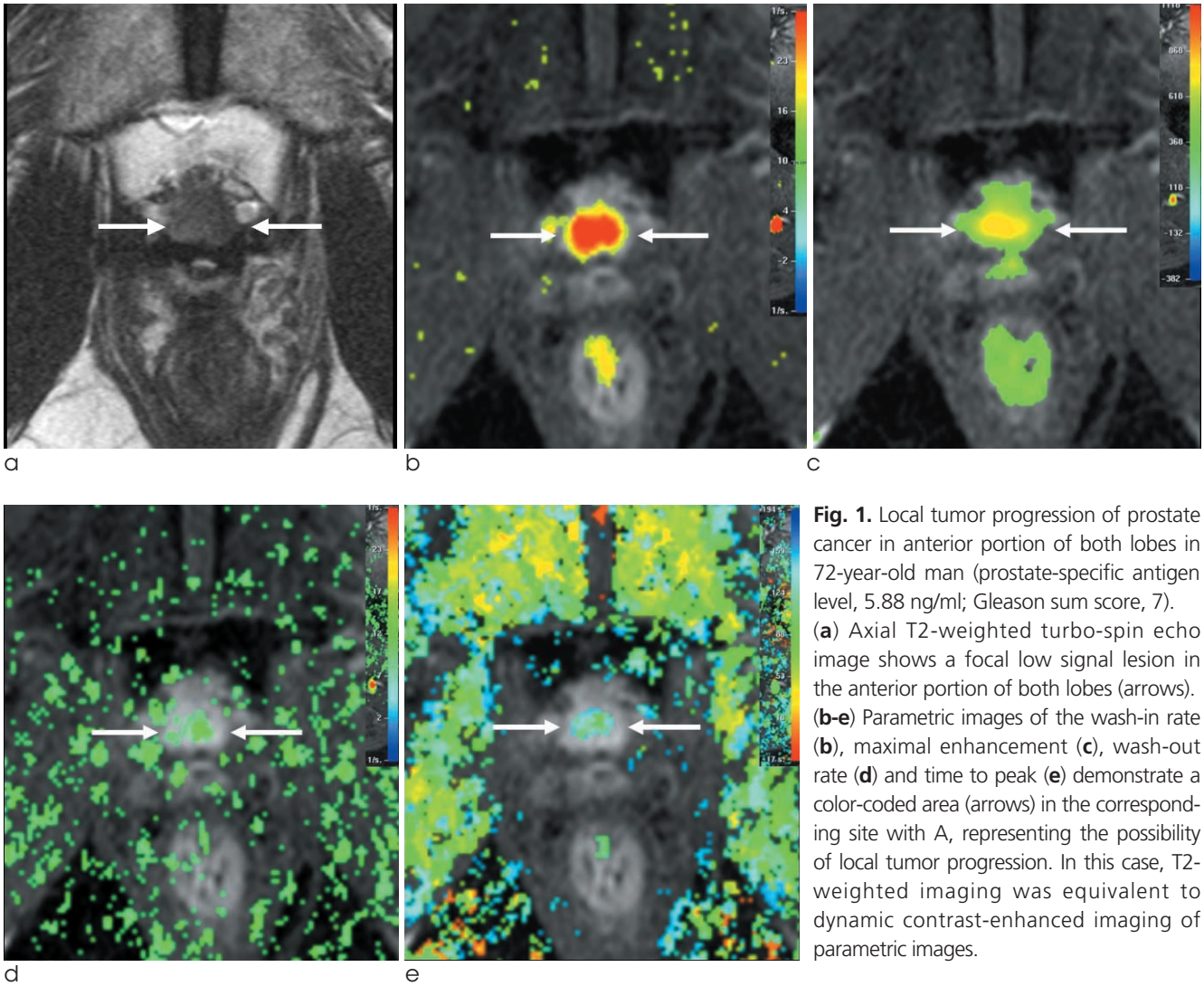

Fig. 1. Local tumor progression of prostate cancer in anterior portion of both lobes in 72-year-old man (prostate-specific antigen level, 5.88 ng/ml; Gleason sum score, 7). (**a**) Axial T2-weighted turbo-spin echo image shows a focal low signal lesion in the anterior portion of both lobes (arrows). (**b-e**) Parametric images of the wash-in rate (**b**), maximal enhancement (**c**), wash-out rate (**d**) and time to peak (**e**) demonstrate a color-coded area (arrows) in the corresponding site with A, representing the possibility of local tumor progression. In this case, T2-weighted imaging was equivalent to dynamic contrast-enhanced imaging of parametric images.

http://dx.doi.org/10.13104/jksmrm.2013.17.3.192

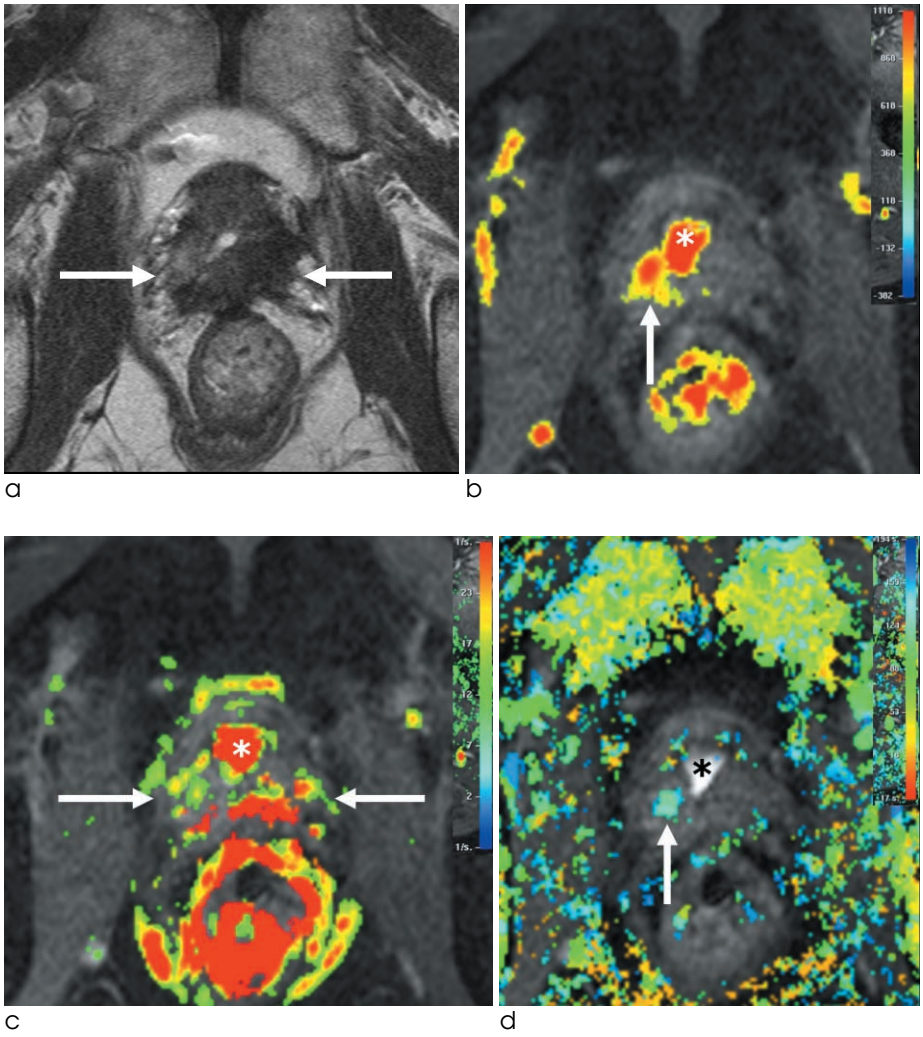

Fig. 2. Local tumor progression of prostate cancer in right lobe at the level of midgland in 69-year-old man (prostate-specific antigen level, 3.50 ng/ml; Gleason sum score, 8).
(**a**) Axial T2-weighted turbo-spin echo image shows diffusely low signal lesion in both lobes at the level of midgland (arrows).
(**b**-**d**) Parametric images of the maximal enhancement (**b**), wash-out rate (**c**) and time to peak (**d**) demonstrate a color-coded area (arrow) in right lobe at the level of midgland, representing the possibility of local tumor progression. Note an asterisk indicates the prostatic urethra. In this case, dynamic contrast-enhanced imaging of parametric images was superior to T2-weighted imaging.

cancer). After HIFU of prostate cancer, early detection of local tumor progression is very important because it affect the determining of second-line treatment that may make an effect on patients' prognosis. Rouviere (9) et al demonstrated that MR imaging could not predict the histologic results of treatment, especially presence of residual cancer foci after HIFU. However, in their study, instead of DCE-MRI, conventional postcontrast MR imaging was used to predict the residual viable tumor.

DCE-MRI was introduced to effectively visualize the pharmacokinetics of gadolinium uptake in the prostate (19). Prostate cancer has been demonstrated to show enhancement patterns that differ from those of benign tissue, and DCE-MRI improves the accuracy of the prostate cancer localization compared with T2WI (20, 21). However, to our knowledge, only a few studies have reported the role of DCE-MRI in the detection of local tumor progression of prostate cancer after HIFU (9–13). Therefore, in our study, DCE-MRI was assessed for the detection of local tumor progression after HIFU. In both readers, the sensitivities of DCE-MRI were 80% and 84%, respectively, which were statistically greater than that of T2WI. These results were in line with previous results with sensitivity of 70–87% (11–13). The specificities of DCE-MRI in both readers were similar with T2WI. The overall accuracies of DCE-MRI in both readers were greater than those of T2WI, but there was not statistically different. For the interobserver agreement, DCE-MRI showed less variability than T2WI.

After HIFU of the prostate, there is complete loss of prostate zonal anatomy and the central gland is not distinguished from the peripheral zone. Furthermore,

prostate tissue may have diffuse or multifocal low-signal area on T2WI (9). These findings may have a difficulty in differentiate between benign tissue and residual or recurrent cancer in remnant prostate tissue. In our study, the sensitivities, specificities and accuracies of T2WI were 57%, 66% and 63% for reader 1 and 61%, 68% and 65% for reader 2, respectively.

In our study, for the detection of local tumor progression of prostate cancer, false-positive results of DCE-MRI were 20% for reader 1 and 16% for reader 2, respectively. As an explainable reason, we did not exclude the central gland in MR imaging analysis due to indistinct zonal anatomy of prostate after HIFU and thus, early enhancement of benign prostate hypertrophy nodules in remnant prostate tissues might mimic local tumor progression.

Our study has some limitations. First, this study is the lack of any histologic gold standard, MR findings being correlated only to TRUS-guided prostate biopsy results. A suspected cancerous lesion in prostate tissue on MR imaging might not be accurately targeted on TRUS-guided prostate biopsy. Conversely, both MR imaging and random biopsy might have missed some residual or recurrent cancer foci. However, a whole-mount pathologic examination of the prostate cannot be obtained from patients treated by HIFU. Therefore, the site-by-site comparison between biopsy and MR findings is a reasonable way of estimating the clinical value of DCE-MRI. Second, this study had small population. For the purpose of producing higher statistical power, higher enrollment numbers would further strengthen our results. Finally, our study did not evaluate quantitative parameters such as volume transfer constant (Ktrans) or fraction of extravascular extracellular volume (Ve) derived from DCE-MRI. Furthermore, diffusion weighted MRI, which is a useful functional imaging method of prostate, was not included in our analysis. Further study should be conducted using those quantitative DCE-MRI parameters or diffusion weighted imaging findings.

In conclusion, for the detection of local tumor progression of prostate cancer after HIFU ablation, DCE-MRI was more sensitive than T2WI, with less interobserver variability than T2WI.

References

1. Aus G, Abbou CC, Bolla M, et al. EAU guidelines on prostate cancer. Eur Urol 2005;48:546-551
2. Aus G. Current status of HIFU and cryotherapy in prostate cancer--a review. Eur Urol 2006;50:927-934; discussion 934
3. Poissonnier L, Chapelon JY, Rouviere O, et al. Control of prostate cancer by transrectal HIFU in 227 patients. Eur Urol 2007;51:381-387
4. Forsythe K, Blacksburg S, Stone N, Stock RG. Intensity-modulated radiotherapy causes fewer side effects than three-dimensional conformal radiotherapy when used in combination with brachytherapy for the treatment of prostate cancer. Int J Radiat Oncol Biol Phys 2012;83:630-635
5. Orsi F, Arnone P, Chen W, Zhang L. High intensity focused ultrasound ablation: a new therapeutic option for solid tumors. J Cancer Res Ther 2010;6:414-420
6. Colombel M, Gelet A. Principles and results of high-intensity focused ultrasound for localized prostate cancer. Prostate Cancer Prostatic Dis 2004;7:289-294
7. Rebillard X, Gelet A, Davin JL, et al. Transrectal high-intensity focused ultrasound in the treatment of localized prostate cancer. J Endourol 2005;19:693-701
8. Gelet A, Chapelon JY, Poissonnier L, et al. Local recurrence of prostate cancer after external beam radiotherapy: early experience of salvage therapy using high-intensity focused ultrasonography. Urology 2004;63:625-629
9. Rouviere O, Lyonnet D, Raudrant A, et al. MRI appearance of prostate following transrectal HIFU ablation of localized cancer. Eur Urol 2001;40:265-274
10. Kirkham AP, Emberton M, Hoh IM, Illing RO, Freeman AA, Allen C. MR imaging of prostate after treatment with high-intensity focused ultrasound. Radiology 2008;246:833-844
11. Kim CK, Park BK, Lee HM, Kim SS, Kim E. MRI techniques for prediction of local tumor progression after high-intensity focused ultrasonic ablation of prostate cancer. AJR Am J Roentgenol 2008;190:1180-1186
12. Ben Cheikh A, Girouin N, Ryon-Taponnier P, et al. MR detection of local prostate cancer recurrence after transrectal high-intensity focused US treatment: preliminary results. J Radiol 2008;89:571-577
13. Punwani S, Emberton M, Walkden M, et al. Prostatic cancer surveillance following whole-gland high-intensity focused ultrasound: comparison of MRI and prostate-specific antigen for detection of residual or recurrent disease. Br J Radiol 2012;85:720-728
14. Goldberg SN, Grassi CJ, Cardella JF, et al. Image-guided tumor ablation: standardization of terminology and reporting criteria. Radiology 2005;235:728-739
15. Engelbrecht MR, Huisman HJ, Laheij RJ, et al. Discrimination of prostate cancer from normal peripheral zone and central gland tissue by using dynamic contrast-enhanced MR imaging. Radiology 2003;229:248-254
16. Futterer JJ, Engelbrecht MR, Huisman HJ, et al. Staging prostate cancer with dynamic contrast-enhanced endorectal MR imaging prior to radical prostatectomy: experienced versus less experienced readers. Radiology 2005;237:541-549
17. Kim JK, Hong SS, Choi YJ, et al. Wash-in rate on the basis of dynamic contrast-enhanced MRI: usefulness for prostate cancer

http://dx.doi.org/10.13104/jksmrm.2013.17.3.192

detection and localization. J Magn Reson Imaging 2005;22:639-646
18. Landis JR, Koch GG. The measurement of observer agreement for categorical data. Biometrics 1977;33:159-174
19. Donahue KM, Weisskoff RM, Parmelee DJ, et al. Dynamic Gd-DTPA enhanced MRI measurement of tissue cell volume fraction. Magn Reson Med 1995;34:423-432
20. Isebaert S, Van den Bergh L, Haustermans K, et al. Multiparametric MRI for prostate cancer localization in correlation to whole-mount histopathology. J Magn Reson Imaging 2012
21. Ocak I, Bernardo M, Metzger G, et al. Dynamic contrast-enhanced MRI of prostate cancer at 3 T: a study of pharmacokinetic parameters. AJR Am J Roentgenol 2007;189:849

대한자기공명의과학회지 17:192-199(2013)

국소적 전립선암의 고강도 집속 초음파 치료 후 국소적 암 재발의 발견과 역동적 조영증강 자기공명영상의 역할

[1]성균관대학교 의과대학 삼성서울병원 영상의학과
[2]성균관대학교 의과대학 삼성서울병원 비뇨기과

박정재[1] · 김찬교[1] · 이현무[2] · 박병관[1] · 박성윤[1]

목적: 국소적 전립선암의 고강도 집속 초음파 치료 후 국소적 암 재발을 발견하는데 있어 역동적 조영증강 자기공명영상의 진단적 능력을 T2 강조영상과 후향적으로 비교하고자 한다.

대상과 방법: 고강도 집속 초음파 치료을 시행 받은 이후 혈중 전립선 특이 항원 수치가 증가한 26명의 환자를 연구에 포함시켰다. 모든 환자는 T2 강조영상과 역동적 조영증강 자기공명영상을 시행 받은 후 경직장 초음파 유도하 조직 검사를 받았으며, 영상 소견과 조직 검사 결과는 전립선을 여섯 구획으로 분리 하여 비교하였다. 조직 검사 결과에서 암 병변이 있는 경우 국소적 암 재발로 정의하였으며, 영상 소견은 두 명의 독립적인 영상의학과 의사가 분석하였다.

결과: 156개의 전립선 구획에서 17명의 환자, 51 구획 (33%)에서 재발암 병변이 발견되었다. 국소적 암 재발의 발견에 있어 역동적 조영증강영상과 T2 강조영상의 민감도는 관찰자 1 에서 각각 80%와 57% ($P < 0.001$), 관찰자 2 에서 각각 84%와 61% ($P < 0.001$) 였다. 두 영상 방법간 특이도와 정확도는 두 관찰자에서 모두 유의한 차이가 없었다 ($P > 0.05$). 관찰자간 일치도에 있어 역동적 조영 증강 영상의 카파값은 0.52, T2 강조 영상의 카파값은 0.21 이었다.

결론: 국소적 전립선암의 고강도 집속 초음파 치료 후 국소적 암 재발을 발견하는데 있어 역동적 조영증강영상은 T2 강조영상보다 더욱 민감하며 관찰자간 일치도 역시 높다.

통신저자 : 김찬교, (135-710) 서울특별시 강남구 일원동 50, 삼성서울병원 영상의학과
Tel. (02) 3410-0516 Fax. (02) 3410-2559 E-mail: chankyokim@skku.edu